UNIVERSITY OF BIRMINGHAM

State Estimation for Communication-Based Train Control Systems with CSMA Protocol

Zou, Lei; Wen, Tao; Wang, Zidong; Chen, Lei; Roberts, Clive

[Link to publication on Research at Birmingham portal](#)

State Estimation for Communication-Based Train Control Systems With CSMA Protocol

Lei Zou[ID], Tao Wen[ID], Zidong Wang[ID], *Fellow, IEEE*, Lei Chen, and Clive Roberts

Abstract—Train positioning is of critical importance for communication-based train control (CBTC) systems. The objective of this paper is to provide an algorithm to generate the precise estimates of the train position and velocity for CBTC systems with carrier-sense multiple access (CSMA) protocol scheduling, thereby improving the accuracy of train positioning as well as the availability of CBTC systems. First, the dynamics of a train with N cars linked by couplers is described based on Newton's motion equations. Then, the transmission model reflecting the behaviors of p-persistent CSMA protocol is presented by using a Bernoulli distributed sequence whose probability distribution is dependent on the number of trains sharing with one communication channel [i.e., $N(k)$]. Furthermore, the value of $N(k)$ is assumed to be unknown but bounded by two known positive integers. The purpose of the problem addressed is to design an estimator, such that the estimation error is exponentially ultimately bounded (with a certain asymptotic upper bound) in mean square subject to the external resistive force. By utilizing the stochastic analysis approach, sufficient conditions are established to guarantee the ultimate boundedness of the estimation error in mean square. For the purpose of designing the desired estimator gains under different requirements (e.g., smallest ultimate bound and fastest decay rate), two optimization problems are solved in terms of linear matrix inequalities. Finally, a simulation example is given to illustrate the effectiveness of the estimator design scheme.

Index Terms—State estimation, communication-based train control systems, CSMA protocol, linear matrix inequalities.

I. INTRODUCTION

THE past decades have witnessed a growing urgency for the safe, efficient and comfortable public mass transit system in major emerging economies including China, India

and Brazil. Owing to the human population explosions in a number of metropolises, metro systems might be the most proper choice to match the increasing demand for low emissions and high capacity transport. For instance, from 2009 to now, more than 80 urban rail transit lines have been or are being built in China and most of them are metro systems. For these metro systems, the highly accurate and dependable train control systems are extremely vital in order to ensure safe operations. In traditional rail systems, the track circuit technology is commonly employed to realize the data exchange between the individual operating train and the train control center [7] and such kind of data exchange has proven to be reliable in early years. However, the track-circuit based control (TBTC) system gives rise to high detection tolerance, thereby leading to long operation headway for each train to make sure there is no possibility for potential collisions. In other words, the track-circuit based technique would probably result in low operation efficiency in the train control center. Moreover, short operation headway of the TBTC system need short length of the track circuit, which would give rise to high cost of the TBTC system.

On the other hand, in response to the rapidly increasing demand for a high efficient urban public transportation system, the communication-based train control (CBTC) system has been developed by utilizing modern radio frequency (RF) technology. Compared with the TBTC system, the CBTC system could achieve much higher detection resolution and moving block by applying wireless data communication (instead of the track-circuit based technology). Up to now, some preliminary results have been reported on the analysis and design issues of CBTC systems [13]–[15], [21]–[23]. For instance, in [4], a multiple-input-multiple-output (MIMO)-assisted handoff scheme for CBTC systems has been proposed in order to reduce handoff latency. The impact of the phenomenon of random packet dropouts has been investigated in [2] on the stability and performances of CBTC systems and, furthermore, two novel schemes to improve the performances of CBTC systems have been developed. In [11], a finite-state Markov channel model has been developed for tunnel channels in CBTC systems by taking the train locations into account to have the accurate channel model. Based on the MIMO-enabled wireless local area networks, a new train-ground communication system has been presented in [19] to improve the handoff latency performance in CBTC system with the consideration of inaccurate channel state information.

In the working process of the CBTC systems, trains should "report" their locations, velocities, identities and other operation information to the train control centers with

sufficient frequency, and then the train control centers notify the corresponding trains of the relevant movement authorities (MAs) according to the working conditions of metro systems. Trains are allowed to keep moving forward with the required velocities after receiving their MAs. Apparently, the exact information about the locations and velocities of trains are of essential importance to the train control centers for the purpose of safe operations. Nevertheless, it is practically difficult to acquire such information because of the "inaccurate measurements" induced by measurement noises and the "unreliable communication" caused by underlying data transmission schemes. In particular, the location of a train for most of CBTC systems is measured by the combination of balises and speed odometers which could cause location errors especially when the train is running on wet or leafy rail tracks. Moreover, the signal transmissions between the trains and the train control center are implemented based on network communication technology which would give rise to data dropouts and communication delays. "inaccurate measurements" and "unreliable communication" will lead to inaccurate train status information and unplanned traction/braking commands, which will affect the safety and Quality of Service (QoS) of CBTC systems. For example, the on-board system will extend the distance between trains to ensure that the train operation will not be affected by the communication delays [5], [10]. Hence, it is of importance to develop certain technology to obtain the precise information about the locations and velocities of trains.

In order to obtain the accurate information of trains, in this paper, we aim to develop a state estimation scheme to generate the estimates about the locations and velocities. The state estimation (or filtering) problems have long been fundamental issues in control theory and a variety of algorithms have been available in the literature. Clearly, the well-developed state estimation techniques would provide a satisfactory means for recovering the true values of the states (e.g. locations and velocities of the trains) from the noisy measurements transmitted from possibly unreliable wireless networks. So far, considerable effort has been devoted to the state estimation issues under different conditions and several effective strategies have been proposed, see [1], [3], [6], [8] and the references therein.

Due to the wireless nature of the communication network of limited bandwidth, the signal exchange between trains and train control centers would suffer from potential risks such as probabilistic signal collisions. Generally speaking, signal collisions in networked systems might occur in case of simultaneous multiple accesses to a shared communication network. As such, communication protocols have been introduced to avoid or mitigate the collisions by orchestrating the transmission order of nodes having permissions to transmit signal. These communication protocols include, but are not limited to, the Round-Robin (RR) protocol [24], [25], the Try-Once-Discard (TOD) protocol [26] and the carrier-sense multiple access (CSMA) protocol (or stochastic communication protocol) [9], [27]. These protocols have been deployed in industry where sensor networks and networked systems are vital parts. In particular, in CBTC systems, the CSMA protocol

is typically utilized to regulate the wireless communication between trains and train control centers.

Summarizing the above discussion, it is of both theoretical significance and practical importance to study the state estimation problem for CBTC systems subject to the CSMA protocol scheduling. This appears to be a challenging task with two essential difficulties identified as follows: 1) how to develop a dynamic model accounting for the random nature of the CBTC system with the CSMA protocol? 2) how to develop appropriate methodology to design the estimator for the CBTC system with the consideration of uncertain nodes (trains) in the CSMA protocol? In this paper, we aim to cope with the identified challenges by examining how the CSMA protocol scheduling alleviates the possible data collisions and designing the state estimator capable of estimating the system states to a prescribed accuracy. *The main contributions of this paper are highlighted as follows. 1) The state estimation problem is, for the first time, investigated for CBTC systems with protocol-based constraints. 2) The influence from the uncertain number of trains sharing with the communication channel is thoroughly studied. 3) The state estimator gains are derived by solving two optimization problems with their aims to obtain the minimum of the asymptotic bound and the fastest decay rate, respectively.*

The rest of this paper is organized as follows. In Section II, the state estimation problem is introduced for a CBTC system with the p-persistent CSMA protocol. In Section III, we deal with the ultimate boundedness problem of the estimation error in mean square by adopting the stochastic analysis approach. Furthermore, two optimization problems are proposed for the design issue of the desired estimator parameters. In Section IV, the effectiveness of the main results is demonstrated by a numerical simulation example. Finally, conclusions are drawn in Section V.

Notations: The notation used here is fairly standard except where otherwise stated. $\mathbb{R}^n$ and $\mathbb{R}^{n \times m}$ denote, respectively, the n dimensional Euclidean space and set of all $n \times m$ real matrices. $\mathbb{N}(\mathbb{N}^+, \mathbb{N}^-)$ denotes the set of integers (nonnegative integers, negative integers). The notation $X \geq Y$ $(X > Y)$, where X and Y are real symmetric matrices, means that $X - Y$ is positive semi-definite (positive definite). Prob$\{\cdot\}$ means the occurrence probability of the event "$\cdot$". $\mathbb{E}\{x\}$ and $\mathbb{E}\{x|y\}$ will, respectively, denote the expectation of the stochastic variable x and expectation of x conditional on y. 0 represents the zero matrix of compatible dimensions. The n-dimensional identity matrix is denoted as I_n or simply I, if no confusion is caused. The shorthand diag$\{\cdots\}$ stands for a block-diagonal matrix. $|a|$ denotes the absolute value of the real number a. $\|A\|$ refers to the norm of a matrix A defined by $\|A\| = \sqrt{\mathrm{trace}(A^T A)}$. M^T represents the transpose of M. Matrices, if they are not explicitly specified, are assumed to have compatible dimensions. The Kronecker delta function $\hbar(a)$ is a binary function that equals 1 if $a = 0$ and equals 0 otherwise.

II. PROBLEM FORMULATION AND PRELIMINARIES

In this section, we first give the overview of the communication-based train control (CBTC) system and
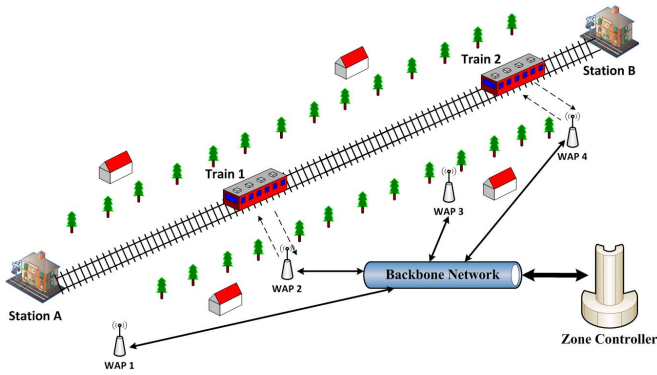
This article has been accepted for inclusion in a future issue of this journal. Content is final as presented, with the exception of pagination.

ZOU *et al.*: STATE ESTIMATION FOR CBTC SYSTEMS WITH CSMA PROTOCOL

3

Fig. 1.   A communication-based train control system.

Fig. 2.   The headway distance of the CBTC system.

introduce some preliminaries related to the dynamic model of the train. Then, we will describe the problem setup.

A. Overview of the CBTC System

As shown in Fig. 1, a typical CBTC system consists of three distinctive parts, namely, the trains, the wayside access points (WAPs) and the Zone Controller (ZC). In such a system, the communication between the train and the WAPs, which is named as *train-ground communication*, is realized through the wireless local area networks (WLANs). The WAPs collect the information about the train status (e.g. the identity, location, direction and velocity) via the train-ground communication, and then transmit the information to the ZC through the backbone network. Based on the information, the ZC knows the location of all the trains in its area and makes the timetables for each train [18]. Unfortunately, due to the "unreliable" communication through the WLANs, the signals collected by WAPs are unavoidably subject to the negative impacts brought from the wireless communication (e.g. protocol-induced constraints). In other words, it is quite common that the ZC cannot obtain the "precise" information about the location and the velocity of the train from the received information directly. As such, particular efforts should be made to design the state estimation algorithm for the ZC to provide a "satisfactory estimation" of the states (location and velocity) of the train.

B. Impacts of Accurate Location and Velocity on CBTC Systems

As a safety-critical system, how to achieve a safe operation is a big issue for CBTC systems. To protect the train and on-board passengers from happening serious hazards or even catastrophes, automated train protection (ATP) systems are employed to ensure the safety of CBTC systems. ATP systems are formed by two parts. The first part is the on-board equipment including the vehicle on-board controller (VOBC), speed sensor, acceleration sensor, balise transmission module and etc. The other is the wayside part, which belongs to the ZC. By fusing the data from the axle counter and track mounted balises, VOBC generates the real-time data about the train's location and speed, and then transmits them to the ZC via the data communication system (DCS). In return, based on these train operation data, including location and speed, the ZC
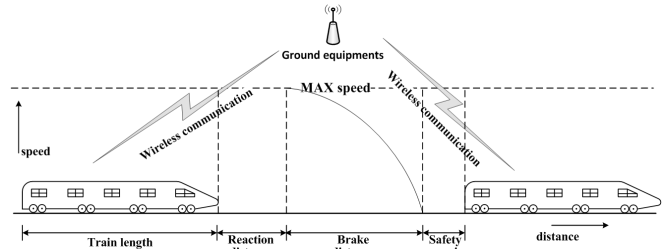
can calculate and send back the limits of movement authorities (LMAs) to trains, which must be respected by every train. Following the received LMAs, VOBC can calculate the safety profile and regulate the train to obey it. If the actual speed is against to the safety profile, braking will be applied. So the precise location and speed data is the fundament in achieving functions for ATP. Low accurate location detection or too big tolerance in measuring speed could lead to errors in generating LMAs or malfunctions in regulating safety profile, which are serious threats for the safety of CBTC systems.

Let's show the impacts of inaccurate location and velocity on the headway of a CBTC system. The typical headway time represents the minimum time interval between two neighboring trains which the signaling will permit, so that the train ahead does not affect a following train. The headway distance denotes the minimum distance between two neighboring trains that the signal will permit. Headway time/distance is the most commonly utilized index to describe the railway capacity within the signaling profession. Reducing the headway time is beneficial to improve the line capacity. The headway distance of a CBTC system is calculated by considering the information about the train location, train speed and the braking performance. The headway time is computed based on the derived headway distance and the train speed. If there is no communication delay in the system, the headway distance could be shown in the Fig. 2.

As shown in Fig. 2, if we could obtain the exact information about the train location and train speed, the headway distance can be calculated as follows [5]:

$$H_D = L_{train} + L_{reaction} + L_{brake} + L_{safe}$$

where L_{train} is the train length, $L_{reaction}$ is the train running distance during the reaction time of on-board system, L_{brake} represents the brake distance at current train speed and L_{safe} denotes the safety margin. However, due to the effects of "inaccurate measurements" and "unreliable communication", the precise location of the train is almost impossible to achieve. For the purpose of safe operation, the train control system always calculates the headway by replacing the train length with the train safety envelope that is defined as the train length at a high confidence level on the premise of safety. The train safety envelope l_S can be computed as follows:

$$l_S = L_{train} + L_{error}$$

where L_{error} is the distance error that is defined as the difference between the actual train location and the measurement.
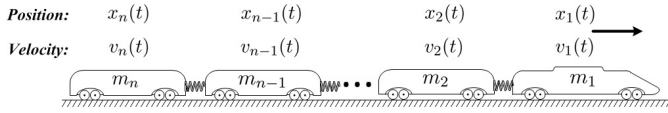
Fig. 3. The diagram of the train.

Assuming that the maximum speed is v_{max}, we can calculate the headway time H_T as follows:

$$H_T = \frac{l_S + L_{reaction} + L_{brake} + L_{safe}}{v_{max}}$$
$$= \frac{L_{train} + L_{error} + L_{reaction} + L_{brake} + L_{safe}}{v_{max}}.$$

Obviously, we can reduce headway time H_T by decreasing the values of L_{error}, which implies that an accurate estimation algorithm for the train position could contribute to the improvement of CBTC systems.

C. Dynamic Model of the Train

Let us consider the dynamics of a train which is modeled by n cars ($n \geq 2$) linked by couplers. The diagram of the train is shown in Fig. 3. The dynamic characteristic of the train is described by the following Newton's motion equations:

$$\begin{cases} \dot{x}_i(t) = v_i(t), \quad i = 1, 2, \cdots, n \\ m_1 \dot{v}_1(t) = u_1(t) - f_1(t) - f_{r,1}(t) \\ m_i \dot{v}_i(t) = u_i(t) + f_{i-1}(t) - f_i(t) - f_{r,i}(t), \\ \qquad\qquad i = 2, 3, \cdots, n-1 \\ m_n \dot{v}_n(t) = u_n(t) + f_{n-1}(t) - f_{r,n}(t) \end{cases} \quad (1)$$

where $x_i(t)$, $v_i(t)$, m_i and $u_i(t)$ ($i = 1, 2, \cdots, n$) represent, respectively, the position, the velocity, the mass and the traction force of the i-th car in the train. $f_i(t)$ ($i = 1, 2, \cdots, n$) denotes the in-train force from the coupler that connects the i-th car and the $(i + 1)$-th car. $f_{r,i}(t)$ ($i = 1, 2, \cdots, n$) represents the resistive force that acts on the i-th car satisfying $|f_{r,i}(t)| \leq \delta_i$ with a known constant positive scalar δ_i.

Remark 1: There are two design schemes for the composition of the traction force: push-pull driving (PPD) design and distributed driving (DD) design. In the PPD design, only the first and the last cars of the train have their traction forces (i.e. $u_2(t) = u_3(t) = \cdots = u_{n-1}(t) = 0$). For the DD design, every car has its own traction force.

Remark 2: The resistive force $f_{r,i}(t)$ ($i = 1, 2, \cdots, n$) exists consistently during the train operation which is caused by certain specified conditions. Generally speaking, the resistive force can be expressed as the sum of the ramp resistance, cure resistance, wind resistance and rolling mechanical resistance. According to [16], the resistive force $f_{r,i}(t)$ ($i = 1, 2, \cdots, n$) could be described as follows:

$$f_{r,i}(t)$$
$$= \begin{cases} (c_0 + c_1 v_1(t)) m_1 + c_2 \sum_{i=1}^{n} m_i v_1^2(t) + \omega_1(t), & i = 1 \\ (c_0 + c_1 v_i(t)) m_i + \omega_i(t), & i = 2, 3, \cdots, n \end{cases}$$

where the coefficients c_0, c_1 and c_2 are obtained by experimental test. $\omega_i(t)$ denotes the ramp resistance of the i-th car satisfying $|\omega_i(t)| \leq \omega_{max}$. Supposing that the speed limit is v_{max} (i.e. $v_i(t) \leq v_{max}$). Hence, it is easy to see that $|f_{r,i}(t)| \leq \delta_i$, where $\delta_1 = (c_0 + c_1 v_{max}) m_1 + c_2 \sum_{i=1}^{n} m_i v_{max}^2 + \omega_{max}$ and $\delta_i = (c_0 + c_1 v_{max}) m_i + \omega_{max}$ ($i = 2, 3, \cdots, n$). As such, in this paper, it is assumed that these resistances are norm-bounded scalars (i.e. $|f_{r,i}(t)| \leq \delta_i$) in order to reflect the reality.

The behavior of couples can be characterized by a spring model where the restoring force is given by

$$f_i(t) = k (x_i(t) - x_{i+1}(t) - \vartheta - l) \quad (2)$$

where $k > 0$ is a known constant positive scalar representing the stiffness coefficient, ϑ denotes the slack length of the couple, and l represents the length of a car.

Denoting

$$\begin{aligned} x(t) &= \begin{bmatrix} x_1(t) \ x_2(t) \ \cdots \ x_n(t) \end{bmatrix}^T, \\ v(t) &= \begin{bmatrix} v_1(t) \ v_2(t) \ \cdots \ v_n(t) \end{bmatrix}^T, \\ \vec{x}(t) &= \begin{bmatrix} x^T(t) v^T(t) \end{bmatrix}^T, \\ \vec{f}_r(t) &= \begin{bmatrix} f_{r,1}(t) \ f_{r,2}(t) \ \cdots \ f_{r,n}(t) \end{bmatrix}^T, \\ h &= \begin{bmatrix} k(\vartheta + l) \ 0 \ 0 \ \cdots \ 0 \ -k(\vartheta + l) \end{bmatrix}^T, \\ \vec{h} &= \begin{bmatrix} 0 \ h^T \end{bmatrix}^T, \\ \mathcal{M} &= \text{diag}\{I_n, \text{diag}\{m_1^{-1}, m_2^{-1}, \cdots, m_n^{-1}\}\}, \end{aligned}$$

the dynamics of the train can be rewritten as follows:

$$\dot{\vec{x}}(t) = \vec{A}\vec{x}(t) + \vec{B}\vec{u}(t) + \vec{E}\vec{f}_r(t) + \mathcal{M}\vec{h} \quad (3)$$

where

$$\vec{A} = \mathcal{M}\begin{bmatrix} 0 & I \\ A & 0 \end{bmatrix}, \quad \vec{B} = \mathcal{M}\begin{bmatrix} 0 \\ B \end{bmatrix}, \quad \vec{E} = \mathcal{M}\begin{bmatrix} 0 \\ -I \end{bmatrix},$$

$$B = \begin{cases} I, & \text{for DD design,} \\ \begin{bmatrix} 1 & 0 & 0 & \cdots & 0 & 0 \\ 0 & 0 & 0 & \cdots & 0 & 1 \end{bmatrix}^T, & \text{for PPD design.} \end{cases}$$

$$A = \begin{bmatrix} -k & k & 0 & 0 & \cdots & \cdots & \cdots & 0 \\ k & -2k & k & 0 & 0 & \cdots & \cdots & 0 \\ 0 & k & -2k & k & 0 & \cdots & \cdots & 0 \\ \vdots & \ddots & \ddots & \ddots & \ddots & \ddots & \cdots & \vdots \\ 0 & \cdots & \cdots & \cdots & k & -2k & k & 0 \\ 0 & \cdots & \cdots & \cdots & \cdots & k & -2k & k \\ 0 & \cdots & \cdots & \cdots & \cdots & \cdots & k & -k \end{bmatrix},$$

$$\vec{u}(t) = \begin{cases} \begin{bmatrix} u_1^T(t) \ u_2^T(t) \ \cdots \ u_n^T(t) \end{bmatrix}^T, & \text{for DD design,} \\ \begin{bmatrix} u_1^T(t) \ u_n^T(t) \end{bmatrix}^T, & \text{for PPD design.} \end{cases}$$

Note that the position and velocity can be easily measured by sensors in the train with a certain sampling period. Assume that the sampling period is T. The measurement output and the signal to be estimated of system (3) are modeled by

$$\begin{cases} \vec{y}(kT) = \tilde{C}\vec{x}(kT) + \omega(kT) \\ \vec{z}(kT) = \tilde{M}\vec{x}(kT) \end{cases} \quad (4)$$

where $\vec{y}(kT)$, $\vec{z}(kT)$ and $\omega(kT)$ ($k \in \mathbb{N}^+$) denote, respectively, the measurement output, the signal to be estimated

and the measurement noise of the k-th sampling instant. $\tilde{C} = \text{diag}\{\tilde{c}_1 I, \tilde{c}_2 I\}$ is the weight matrix of the measurement data. The constants $\tilde{c}_1$ and $\tilde{c}_2$ represent the weights of the position and velocity, respectively. $\tilde{M}$ is a known matrix with appropriate dimensions. Without loss of generality, it is assumed that $\omega(kT)$ is the zero-mean Gaussian white noise with covariance $\Omega \triangleq \bar{\Omega}^T \bar{\Omega}$.

For technical convenience, we now transform the system (3) into a discrete-time model according the sampling period T. Suppose that $\tilde{u}(k) = \vec{u}(kT)$ and $\tilde{f}_r(k) = \vec{f}_r(kT)$ for $kT \le t < (k+1)T$. It follows from (3) and (4) that

$$\begin{cases} \tilde{x}(k+1) = \tilde{A}\tilde{x}(k) + \tilde{B}\tilde{u}(k) + \tilde{E}\tilde{f}_r(k) + \tilde{H}\vec{h} \\ \tilde{y}(k) = \tilde{C}\tilde{x}(k) + \tilde{\omega}(k) \\ \tilde{z}(k) = \tilde{M}\tilde{x}(k) \end{cases} \tag{5}$$

where

$$\tilde{x}(k) = \vec{x}(kT), \quad \tilde{u}(k) = \vec{u}(kT), \quad \tilde{f}_r(k) = \vec{f}_r(kT),$$
$$\tilde{y}(k) = \vec{y}(kT), \quad \tilde{z}(k) = \vec{z}(kT), \quad \tilde{\omega}(k) = \omega(kT), \quad \tilde{A} = e^{\bar{A}T},$$
$$\tilde{B} = \int_0^T e^{\bar{A}t} dt \vec{B}, \quad \tilde{H} = \int_0^T e^{\bar{A}t} dt \mathcal{M}, \quad \tilde{E} = \int_0^T e^{\bar{A}t} dt \vec{E}.$$

D. Transmission Model Based on the CSMA Protocol

Let us now consider the data transmission via the train-ground communication. In this paper, the communication between each WAP and trains in its coverage area is scheduled by certain protocol according to the IEEE 802.11p standard. As show in [20], the IEEE 802.11p is a draft amendment to the IEEE 802.11 standards and has been applied to fast changing vehicular networks including the train-ground communication in CBTC systems. Furthermore, IEEE 802.11p could be modeled as the p-persistent CSMA protocol [12]. In such a protocol, *only one train* is permitted to communicate with the corresponding WAP at each transmission instant. Each train would transmit the signal with the probability p ($0 < p \le 1$) if the communication channel is sensed idle. Otherwise, the train waits until next available transmission instant. For the sake of simplicity, we assume that the measurement output is transmitted at each sampling instant. Then, the transmission model of the system (5) subject to the p-persistent CSMA protocol is given by

$$\bar{y}(k) = \alpha(k)\tilde{y}(k) \tag{6}$$

where $\bar{y}(k)$ represents the measurement signal received by the ZC via WLANs and $\alpha(k) \in \{0, 1\}$ is a Bernoulli distributed stochastic variable indicating whether the communication channel is idle at present. We assumed that $\alpha(k)$ is unrelated to the measurement noise $\tilde{\omega}(k)$. The probability distribution of $\alpha(k)$ can be calculated as follows [9]:

$$\begin{cases} \text{Prob}\{\alpha(k) = 1\} = p(1-p)^{N(k)-1}, \\ \text{Prob}\{\alpha(k) = 0\} = 1 - p(1-p)^{N(k)-1}, \end{cases} \tag{7}$$

where $N(k)$ is the number of trains in the coverage area of certain WAP at time k. Obviously, $N(k)$ is a bounded integer variable due to the fact that trains must keep a distance far enough between each other in order to guarantee safety.

Assuming that $\underline{N} \le N(k) \le \overline{N}$ where $\overline{N}$ and $\underline{N}$ are known constant positive integers, it follows from (7) that

$$\begin{cases} \bar{\alpha} \triangleq \mathbb{E}\{\alpha(k)\} = \bar{p} + \Delta_1(k) \\ \mathbb{E}\left\{(\alpha(k) - \bar{\alpha})^2\right\} = \hat{p} + \Delta_2(k) \end{cases} \tag{8}$$

where

$$\bar{p} = \frac{1}{2}\left(p(1-p)^{\underline{N}-1} + p(1-p)^{\overline{N}-1}\right),$$
$$\hat{p} = \frac{1}{2}\left(p(1-p)^{\underline{N}-1}\left(1 - p(1-p)^{\underline{N}-1}\right)\right.$$
$$\left. + p(1-p)^{\overline{N}-1}\left(1 - p(1-p)^{\overline{N}-1}\right)\right),$$
$$\Delta_1(k) = p(1-p)^{N(k)-1} - \bar{p},$$
$$\Delta_2(k) = p(1-p)^{N(k)-1}\left(1 - p(1-p)^{N(k)-1}\right) - \hat{p}.$$

It is easy to verify that

$$\begin{cases} |\Delta_1(k)| \le \bar{\Delta}_p \\ |\Delta_2(k)| \le \hat{\Delta}_p \end{cases} \tag{9}$$

where

$$\bar{\Delta}_p = \frac{p(1-p)^{\underline{N}-1} - p(1-p)^{\overline{N}-1}}{2}$$
$$\hat{\Delta}_p = \frac{1}{2}\left(p(1-p)^{\underline{N}-1}\left(1 - p(1-p)^{\underline{N}-1}\right)\right.$$
$$\left. - p(1-p)^{\overline{N}-1}\left(1 - p(1-p)^{\overline{N}-1}\right)\right).$$

Remark 3: It is worth mentioning that the identity information of each train is transmitted to the ZC simultaneously in the transmission. As such, the value of the stochastic variable $\alpha(k)$ is available to the ZC, but the exact number of trains $N(k)$ in the coverage area of a WAP could not be obtained.

E. Structure of the Estimator

Consider the following state estimator for the discrete-time stochastic system (5) with the CSMA protocol scheduling (6):

$$\begin{cases} \hat{x}(k+1) = \tilde{A}\hat{x}(k) + \tilde{B}\tilde{u}(k) + \tilde{H}\vec{h} \\ \qquad\qquad + K\left(\bar{y}(k) - \alpha(k)\tilde{C}\hat{x}(k)\right) \\ \hat{z}(k) = \tilde{M}\hat{x}(k) \end{cases} \tag{10}$$

where K is the estimator parameter to be designed.

Let the estimation error be $e(k) \triangleq x(k) - \hat{x}(k)$ and the output estimation error be $\tilde{z}(k) \triangleq z(k) - \hat{z}(k)$. Then, the estimation error dynamics for the discrete-time system (5) is obtained as follows:

$$\begin{cases} e(k+1) = \left(\tilde{A} - \alpha(k)K\tilde{C}\right)e(k) - \alpha(k)K\tilde{\omega}(k) + \tilde{E}\tilde{f}_r(k) \\ \qquad = \left(\tilde{A} - (\bar{p} + \Delta_1(k) + \tilde{\alpha}(k))K\tilde{C}\right)e(k) \\ \qquad\quad - \left(\bar{p} + \Delta_1(k) + \tilde{\alpha}(k)\right)K\tilde{\omega}(k) + \tilde{E}\tilde{f}_r(k) \\ \tilde{z}(k) = \tilde{M}e(k) \end{cases} \tag{11}$$

where $\tilde{\alpha}(k) = \alpha(k) - \bar{\alpha}(k)$.

Now, let us introduce the following definition that is necessary for the problem statement.

Definition 1: The dynamics of the estimation error $e(k)$ (i.e. the solution of system (11)) is said to be exponentially

ultimately bounded in mean square if there exist constants $\mu \in [0, 1)$, $\theta > 0$ and $\delta > 0$ such that

$$\mathbb{E}\left\{\|e(k)\|^2 | e(0)\right\} \leq \mu^k \theta + \delta. \tag{12}$$

We denote by μ and δ, respectively, the decay rate and the asymptotic upper bound of $\mathbb{E}\left\{\|e(k)\|^2\right\}$.

We are now in the position to state the main goal of this paper. We are interested in investigating the ultimate boundedness of the estimation error dynamics in mean square and designing the estimator gain matrix according to two performance optimization problems. More specifically, our objectives in this paper are to

1) derive sufficient conditions for the dynamical system (11) under which the ultimate boundedness is guaranteed for the estimation error $e(k)$ in mean square.
2) design the estimator gain matrix K in order to obtain the minimization of the ultimate bound and the fastest decay rate of the output estimation error.

III. MAIN RESULTS

In this section, the ultimate boundedness is analyzed for the estimation error $e(k)$ in mean square. Before proceeding further, we introduce the following lemma which will be needed for the derivation of our main results.

Lemma 1 (Schur Complement Lemma): Given constant matrices $\mathcal{S}_1$, $\mathcal{S}_2$ and $\mathcal{S}_3$ where $\mathcal{S}_1 = \mathcal{S}_1^T$ and $0 < \mathcal{S}_2 = \mathcal{S}_2^T$, then $\mathcal{S}_1 + \mathcal{S}_3^T \mathcal{S}_2^{-1} \mathcal{S}_3 < 0$ if and only if

$$\begin{bmatrix} \mathcal{S}_1 & \mathcal{S}_3^T \\ * & -\mathcal{S}_2 \end{bmatrix} < 0, \quad \text{or} \quad \begin{bmatrix} -\mathcal{S}_2 & \mathcal{S}_3 \\ * & \mathcal{S}_1 \end{bmatrix} < 0. \tag{13}$$

A. Ultimate Boundedness Analysis of the Estimation Error

The following theorem provides a sufficient condition under which the dynamics of the estimation error is exponentially ultimately bounded in mean square.

Theorem 1: Let the estimator parameter K be given. Assume that there exist a positive definite matrices $P \in \mathbb{R}^{2n \times 2n}$, three positive scalars λ_1, λ_2 and γ satisfying

$$\bar{\Gamma} \triangleq \begin{bmatrix} \bar{\Gamma}_{11} & \bar{\Gamma}_{12} & \bar{\Gamma}_{13} \\ * & \bar{\Gamma}_{22} & \bar{\Gamma}_{23} \\ * & * & \bar{\Gamma}_{33} \end{bmatrix} < 0 \tag{14}$$

where

$$\bar{\Gamma}_{11} = (\tilde{A} - \bar{p}K\tilde{C})^T P (\tilde{A} - \bar{p}K\tilde{C}) - (1 - \gamma)P + \bar{\Delta}_p^2 \lambda_1 I$$
$$\qquad + (\hat{p} + \hat{\Delta}_p))\tilde{C}^T K^T P K \tilde{C},$$
$$\bar{\Gamma}_{12} = -(\tilde{A} - \bar{p}K\tilde{C})^T P K \tilde{C}, \quad \bar{\Gamma}_{13} = (\tilde{A} - \bar{p}K\tilde{C})^T P \tilde{E},$$
$$\bar{\Gamma}_{22} = \tilde{C}^T K^T P K \tilde{C} - \lambda_1 I, \quad \bar{\Gamma}_{23} = -\tilde{C}^T K^T P \tilde{E},$$
$$\bar{\Gamma}_{33} = \tilde{E}^T P \tilde{E} - \lambda_2 I.$$

Then, the dynamics of the estimation error $e(k)$ is ultimately bounded in mean square subject to the measurement noise $\tilde{\omega}(k)$ and the resistive force $\tilde{f}_r(k)$.

Proof: To analyze the ultimate boundedness of the estimation error $e(k)$, we choose the following Lyapunov-like function:

$$V(k) = e^T(k) P e(k). \tag{15}$$

The corresponding difference of $V(k)$ along the trajectory of system (11) can be calculated as follows:

$$\Delta V(k)$$
$$\triangleq e^T(k+1) P e(k+1) - e^T(k) P e(k)$$
$$= \Big((\tilde{A} - \bar{p}K\tilde{C})e(k) - \Delta_1(k)K\tilde{C}e(k) - \tilde{\alpha}(k)K\big(\tilde{C}e(k)$$
$$\quad + \tilde{\omega}(k)\big) - (\bar{p} + \Delta_1(k))K\tilde{\omega}(k) + \tilde{E}\tilde{f}_r(k) \Big)^T P \Big((\tilde{A} - \bar{p}$$
$$\quad \times K\tilde{C})e(k) - \Delta_1(k)K\tilde{C}e(k) - \tilde{\alpha}(k)K\big(\tilde{C}e(k) + \tilde{\omega}(k)\big)$$
$$\quad + \tilde{E}\tilde{f}_r(k) - (\bar{p} + \Delta_1(k))K\tilde{\omega}(k) \Big) - e^T(k) P e(k). \tag{16}$$

Since $\mathbb{E}\{\tilde{\omega}(k)\} = 0$ and $\mathbb{E}\{\tilde{\omega}(k)\tilde{\omega}^T(k)\} = \Omega$, it follows from (16) that

$$\mathbb{E}\{\Delta V(k)\}$$
$$= \mathbb{E}\Big\{ e^T(k)\Big((\tilde{A} - \bar{p}K\tilde{C})^T P (\tilde{A} - \bar{p}K\tilde{C}) - P \Big) e(k) + \Delta_1^2(k)$$
$$\quad \times e^T(k)\tilde{C}^T K^T P K \tilde{C} e(k) - 2\Delta_1(k)e^T(k)(\tilde{A} - \bar{p}K\tilde{C})^T$$
$$\quad \times P K \tilde{C} e(k) + (\hat{p} + \Delta_2(k))\big(e^T(k)\tilde{C}^T K^T P K \tilde{C} e(k)$$
$$\quad + \tilde{\omega}^T(k)K^T P K \tilde{\omega}(k)\big) + \tilde{f}_r^T(k)\tilde{E}^T P \tilde{E}\tilde{f}_r(k) + (\bar{p}$$
$$\quad + \Delta_1(k))^2 \tilde{\omega}^T(k)K^T P K \tilde{\omega}(k) + 2e^T(k)(\tilde{A} - \bar{p}K\tilde{C})^T P$$
$$\quad \times \tilde{E}\tilde{f}_r(k) - 2\Delta_1(k)e^T(k)\tilde{C}^T K^T P \tilde{E}\tilde{f}_r(k) \Big\}$$
$$= \mathbb{E}\{\vartheta^T(k)\Gamma\vartheta(k)\} + \big((\bar{p} + \Delta_1(k))^2 + \hat{p}$$
$$\quad + \Delta_2(k)\big)\text{tr}\{\bar{\Omega}^T K^T P K \bar{\Omega}\} \tag{17}$$

where

$$\Gamma_{11} = (\tilde{A} - \bar{p}K\tilde{C})^T P (\tilde{A} - \bar{p}K\tilde{C}) - P$$
$$\qquad + (\hat{p} + \Delta_2(k))\tilde{C}^T K^T P K \tilde{C},$$
$$\Gamma_{12} = -(\tilde{A} - \bar{p}K\tilde{C})^T P K \tilde{C}, \quad \Gamma_{13} = (\tilde{A} - \bar{p}K\tilde{C})^T P \tilde{E},$$
$$\Gamma_{22} = \tilde{C}^T K^T P K \tilde{C}, \quad \Gamma_{23} = -\tilde{C}^T K^T P \tilde{E}, \quad \Gamma_{33} = \tilde{E}^T P \tilde{E},$$
$$\vartheta(k) = \begin{bmatrix} e(k) \\ \Delta_1(k)e(k) \\ \tilde{f}_r(k) \end{bmatrix}, \quad \Gamma = \begin{bmatrix} \Gamma_{11} & \Gamma_{12} & \Gamma_{13} \\ * & \Gamma_{22} & \Gamma_{23} \\ * & * & \Gamma_{33} \end{bmatrix}.$$

Noting that $|\Delta_1(k)| \leq \bar{\Delta}_p$ and $|\Delta_2(k)| \leq \hat{\Delta}_p$, it can be derived from (17) that

$$\mathbb{E}\{\Delta V(k)\} \leq \mathbb{E}\{\vartheta^T(k)\Gamma\vartheta(k)\} + \varepsilon\text{tr}\{\bar{\Omega}^T K^T P K \bar{\Omega}\} \tag{18}$$

where $\varepsilon = p(1 - p)^{\frac{N-1}{2}}$. Moreover, one can infer from (18) that

$$\mathbb{E}\{\Delta V(k)\}$$
$$\leq \mathbb{E}\{\vartheta^T(k)\Gamma\vartheta(k)\} + \varepsilon\text{tr}\{\bar{\Omega}^T K^T P K \bar{\Omega}\} - \lambda_2 \|\tilde{f}_r(k)\|^2$$
$$\quad + \lambda_1 \Delta_1^2(k)\|e(k)\|^2 - \lambda_1 \Delta_1^2(k)\|e(k)\|^2 + \lambda_2 \|\tilde{f}_r(k)\|^2$$
$$\quad + \varepsilon\text{tr}\{\bar{\Omega}^T K^T P K \bar{\Omega}\}$$
$$\leq -\gamma\mathbb{E}\{V(k)\} + \bar{\varepsilon} \tag{19}$$

where $\bar{\varepsilon} = \varepsilon\text{tr}\{\bar{\Omega}^T K^T P K \bar{\Omega}\} + \lambda_2 \sum_{i=1}^{n} \delta_i^2$. Hence, for any scalar $\rho > 0$, it follows that

$$\mathbb{E}\{\rho^{k+1} V(k+1)\} - \mathbb{E}\{\rho^k V(k)\}$$
$$= \rho^{k+1}\big(\mathbb{E}\{V(k+1)\} - \mathbb{E}\{V(k)\}\big) + \rho^k(\rho - 1)\mathbb{E}\{V(k)\}$$
$$\leq \rho^k(\rho - 1 - \rho\gamma)\mathbb{E}\{V(k)\} + \rho^{k+1}\bar{\varepsilon}. \tag{20}$$

It is obvious that $0 < \gamma < 1$. Letting $\rho = \rho_0 = \frac{1}{1-\gamma}$ and summing up both sides of (20) from 0 to $\kappa - 1$ with respect to κ, we obtain

$$\mathbb{E}\{\rho_0^\kappa V(t)\} - \mathbb{E}\{V(0)\} \leq \frac{\rho_0(1 - \rho_0^\kappa)}{1 - \rho_0}\bar{\varepsilon} \qquad (21)$$

which implies that

$$\mathbb{E}\{V(\kappa)\} \leq \rho_0^{-\kappa}\left(\mathbb{E}\{V(0)\} + \frac{\rho_0}{1 - \rho_0}\bar{\varepsilon}\right) - \frac{\rho_0}{1 - \rho_0}\bar{\varepsilon}$$
$$= (1 - \gamma)^\kappa\left(\mathbb{E}\{V(0)\} - \frac{\bar{\varepsilon}}{\gamma}\right) + \frac{\bar{\varepsilon}}{\gamma}. \qquad (22)$$

Finally, it follows readily from Definition 1 that the error dynamical system (11) is exponentially ultimately bounded in mean square where the asymptotic upper bound of the estimation error can be computed as $\frac{\bar{\varepsilon}}{\gamma \lambda_{\min}\{P\}}$. The proof is complete. ∎

Remark 4: In Theorem 1, a sufficient condition has been derived under which the estimation error $e(k)$ is exponentially ultimately bounded in mean square subject to the measurement noise $\tilde{\omega}(k)$ and the resistive force $\tilde{f}_r(k)$. It is worth mentioning that a guaranteed ultimate bound of the estimation error dynamics can be associated with a kind of estimation performance about the "attenuation" against the effect of perturbations. On the other hand, it can be seen from (14) that the decay rate of the estimation error (i.e. $1-\gamma$) should be large enough to guarantee the ultimate boundedness of $e(k)$. From a practical point of view, the decay rate and the ultimate bound in mean square can be regarded as two important performance indices for the estimation performance.

B. Optimization Problems

In this subsection, we focus our attention on design problem of the state estimator gain matrix k by solving two optimization problems.

1) Optimization Problem 1: Minimization of the ultimate bound in mean square of the estimation error dynamics for most accurate estimate performance.

Corollary 1: For system (11), let a scalar $1 > \theta > 0$ be given. Suppose that there exist two positive definite matrices $P \in \mathbb{R}^{2n \times 2n}$, $Q \in \mathbb{R}^{2n \times 2n}$, two positive scalars λ_1, λ_2, and a matrix $\mathcal{K} \in \mathbb{R}^{2n \times 2n}$ satisfying

$$\Xi = \begin{bmatrix} \Xi_{11} & 0 & 0 & \Xi_{14} & \Xi_{15} \\ * & \Xi_{22} & 0 & \Xi_{24} & 0 \\ * & * & \Xi_{33} & \Xi_{34} & 0 \\ * & * & * & \Xi_{44} & 0 \\ * & * & * & * & \Xi_{55} \end{bmatrix} < 0 \qquad (23)$$

$$\begin{bmatrix} -Q & \bar{\Omega}^T \mathcal{K}^T \\ * & -P \end{bmatrix} < 0 \qquad (24)$$

$$P \geq \tilde{M}^T \tilde{M} \qquad (25)$$

where

$$\Xi_{11} = \bar{\Delta}_p^2 \lambda_1 I - \theta P, \quad \Xi_{14} = \tilde{A}^T P - \bar{p}\tilde{C}^T \mathcal{K}^T, \quad \Xi_{15} = \tilde{C}^T \mathcal{K}^T,$$
$$\Xi_{22} = -\lambda_1 I, \quad \Xi_{24} = -\tilde{C}^T \mathcal{K}^T, \quad \Xi_{33} = -\lambda_2 I, \quad \Xi_{34} = \tilde{E}^T P,$$
$$\Xi_{44} = -P, \quad \Xi_{55} = -\frac{P}{\hat{p} + \hat{\Delta}_p}, \quad \varepsilon = p(1-p)^{N-1}.$$

Then, the dynamics of the estimation error $e(k)$ is ultimately bounded in mean square subject to the measurement noise $\tilde{\omega}(k)$ and the resistive force $\tilde{f}_r(k)$. Furthermore, the decay rate of the estimation error is less than θ, and the minimum of the asymptotic upper bound of $\mathbb{E}\{\|e(k)\|^2\}$ can be derived by solving the following minimization problem

$$\min\left\{\varepsilon \text{tr}\{Q\} + \lambda_2 \sum_{i=1}^n \delta_i^2\right\} \qquad (26)$$

subject to the matrix inequality constraints (23)-(25). The desired state estimator gain can be obtained by

$$K = P^{-1}\mathcal{K}. \qquad (27)$$

Proof: Based on the Schur Complement Lemma (Lemma 1) and the desired state estimator gain in (27), it can be concluded that the inequality (14) holds with the condition $\gamma = 1 - \theta$ if and only if the inequality (23) is satisfied. Hence, it follows from Theorem 1 that the dynamics of the estimation error $e(k)$ is ultimately bounded in mean square.

On the other hand, along similar lines as the proof of Theorem 1, it can be derived that

$$\mathbb{E}\{V(k)\} \leq \theta^k\left(\mathbb{E}\{V(0)\} - \frac{\bar{\varepsilon}}{1 - \theta}\right) + \frac{\bar{\varepsilon}}{1 - \theta} \qquad (28)$$

where

$$\bar{\varepsilon} = \varepsilon \text{tr}\{\bar{\Omega}^T \mathcal{K}^T P^{-1} \mathcal{K}\bar{\Omega}\} + \lambda_2 \sum_{i=1}^n \delta_i^2.$$

Moreover, one can infer from (24) that

$$\bar{\Omega}^T \mathcal{K}^T P^{-1} \mathcal{K}\bar{\Omega} \leq Q. \qquad (29)$$

Therefore, it follows from (28) and (29) that

$$\mathbb{E}\{V(k)\} \leq \theta^k \mathbb{E}\{V(0)\} - \frac{\theta^k \bar{\varepsilon}}{1-\theta} + \frac{\varepsilon \text{tr}\{Q\} + \lambda_2 \sum_{i=1}^n \delta_i^2}{1-\theta}. \qquad (30)$$

Since $\|\tilde{z}(k)\|^2 \leq V(k)$, we have

$$\mathbb{E}\{\|\tilde{z}(k)\|^2\}$$
$$\leq \mathbb{E}\{V(k)\}$$
$$\leq \theta^k\left(\mathbb{E}\{V(0)\} - \frac{\bar{\varepsilon}}{1-\theta}\right) + \frac{\varepsilon \text{tr}\{Q\} + \lambda_2 \sum_{i=1}^n \delta_i^2}{1-\theta}. \qquad (31)$$

As such, we can conclude that the asymptotic bound of $\mathbb{E}\{\|e(k)\|^2\}$ is

$$\frac{\varepsilon \text{tr}\{Q\} + \lambda_2 \sum_{i=1}^n \delta_i^2}{1-\theta}$$

and the minimum of this asymptotic bound can be derived by minimizing

$$\varepsilon \text{tr}\{Q\} + \lambda_2 \sum_{i=1}^n \delta_i^2$$

which is equivalent to (26). The proof is complete. ∎

This article has been accepted for inclusion in a future issue of this journal. Content is final as presented, with the exception of pagination.

8

IEEE TRANSACTIONS ON INTELLIGENT TRANSPORTATION SYSTEMS

2) Optimization Problem 2: Optimization of the decay rate of the estimation error dynamics for fastest convergence performance.

Corollary 2: For system (11), let a scalar $\varpi > 0$ be given. Suppose that a nonsingular matrix $R \in \mathbb{R}^{2n \times 2n}$, four positive scalars $\lambda_1 > 0$, $\lambda_2 > 0$, $\bar{\gamma} > 1$, $\varrho > 0$, and a matrix $\mathcal{K} \in \mathbb{R}^{2n \times 2n}$ satisfying

$$\Theta = \begin{bmatrix} \Theta_{11} & 0 & 0 & \Theta_{14} & \Theta_{15} \\ * & \Theta_{22} & 0 & \Theta_{24} & 0 \\ * & * & \Theta_{33} & \Theta_{34} & 0 \\ * & * & * & \Theta_{44} & 0 \\ * & * & * & * & \Theta_{55} \end{bmatrix} < 0 \qquad (32)$$

$$\begin{bmatrix} -\varpi(\bar{\gamma} - 1) + \lambda_2 \sum_{i=1}^{n} \delta_i^2 & \Upsilon \\ * & -\varepsilon^{-1}I \end{bmatrix} < 0 \qquad (33)$$

$$\begin{bmatrix} -R - R^T + \varrho I & \bar{\gamma} \tilde{M}^T \\ * & -\varrho I \end{bmatrix} \le 0 \qquad (34)$$

where

$\Theta_{11} = -R - R^T + \bar{\gamma} I + \bar{\Delta}_p^2 \lambda_1 I, \quad \Theta_{14} = \tilde{A}^T R^T - \bar{p}\tilde{C}^T \mathcal{K}^T,$

$\Theta_{15} = \tilde{C}^T \mathcal{K}^T, \Theta_{22} = -\lambda_1 I, \quad \Theta_{24} = -\tilde{C}^T \mathcal{K}^T, \Theta_{33} = -\lambda_2 I,$

$\Theta_{34} = \tilde{E}^T R^T, \quad \Theta_{44} = -I, \quad \Theta_{55} = -\dfrac{I}{\hat{p} + \hat{\Delta}_p},$

$\Lambda_i = \begin{bmatrix} \hbar(i-1) \ \hbar(i-2) \ \cdots \ \hbar(i-2n) \end{bmatrix}^T,$

$\Upsilon = \begin{bmatrix} \Lambda_1^T \bar{\Omega}^T \mathcal{K}^T \ \Lambda_2^T \bar{\Omega}^T \mathcal{K}^T \ \cdots \ \Lambda_{2n}^T \bar{\Omega}^T \mathcal{K}^T \end{bmatrix},$

$\varepsilon = p(1-p)^{\underline{N}-1},$

and $\hbar(\cdot) \in \{0, 1\}$ is the Kronecker delta function. Then, the dynamics of the estimation error $\tilde{z}(k)$ is exponentially ultimately bounded in mean square with the decay rate $\bar{\gamma}^{-1}$ subject to the measurement noise $\tilde{\omega}(k)$ and the resistive force $\tilde{f}_r(k)$. Furthermore, the upper bound of $\mathbb{E}\{\|\tilde{z}(k)\|^2\}$ is less than ϖ and the optimum of the decay rate can be derived by solving the following maximization problem

$$\max\{\bar{\gamma}\} \qquad (35)$$

subject to the matrix inequality constraints (32)-(34). The desired state estimator gain can be obtained by

$$K = R^{-1}\mathcal{K}. \qquad (36)$$

Proof: Choose the following Lyapunov-like function:

$$V(k) = e^T(k) R^T R e(k). \qquad (37)$$

Along the similar lines as the proof of Theorem 1, it can be derived from (36) that

$$\mathbb{E}\{\Delta V(k)\} = \mathbb{E}\{\vartheta^T(k)\bar{\Theta}\vartheta(k)\} - \left(1 - \frac{1}{\bar{\gamma}}\right)\mathbb{E}\{V(k)\} + \hat{\varepsilon} \qquad (38)$$

where

$$\bar{\Theta} = \text{diag}\left\{-\bar{\gamma}^{-1}R^T R + \bar{\Delta}_p^2 \lambda_1 I, -\lambda_1 I, -\lambda_2 I\right\}$$

$$+ \begin{bmatrix} \Theta_{14} \\ \Theta_{24} \\ \Theta_{34} \end{bmatrix}\begin{bmatrix} \Theta_{14} \\ \Theta_{24} \\ \Theta_{34} \end{bmatrix}^T + \frac{1}{\hat{p} + \hat{\Delta}_p}\begin{bmatrix} \Theta_{15} \\ 0 \\ 0 \end{bmatrix}\begin{bmatrix} \Theta_{15} \\ 0 \\ 0 \end{bmatrix}^T,$$

$$\hat{\varepsilon} = \varepsilon\text{tr}\{\bar{\Omega}^T \mathcal{K}^T \mathcal{K}\bar{\Omega}\} + \lambda_2 \sum_{i=1}^{n} \delta_i^2$$

$$= \varepsilon \sum_{i=1}^{2n} \Lambda_i^T \bar{\Omega}^T \mathcal{K}^T \mathcal{K}\bar{\Omega}\Lambda_i + \lambda_2 \sum_{i=1}^{n} \delta_i^2$$

$$= \varepsilon\Upsilon\Upsilon^T + \lambda_2 \sum_{i=1}^{n} \delta_i^2.$$

Since

$$-\bar{\gamma}^{-1}R^T R \le -R^T - R + \bar{\gamma} I,$$

it follows from the Schur Complement Lemma (Lemma 1), (32) and (38) that $\bar{\Theta} < 0$, which implies that

$$\mathbb{E}\{\Delta V(k)\} \le -\left(1 - \frac{1}{\bar{\gamma}}\right)\mathbb{E}\{V(k)\} + \hat{\varepsilon}. \qquad (39)$$

Then, it can be concluded from Theorem 1 that the dynamics of the estimation error $e(k)$ is ultimately bounded in mean square.

On the other hand, one can infer from (34) that

$$R^T R \ge \varrho\left(R + R^T - \varrho I\right) \ge \bar{\gamma}^2 \tilde{M}^T \tilde{M}. \qquad (40)$$

Hence, we have

$$\mathbb{E}\{\|\tilde{z}(k)\|^2\} \le \mathbb{E}\{V(k)\}$$

$$\le \bar{\gamma}^{-k-2}\left(E\{V(0)\} - \frac{\bar{\gamma}}{\bar{\gamma} - 1}\right) + \frac{\hat{\varepsilon}}{\bar{\gamma} - 1}. \qquad (41)$$

According to the inequality (33) that

$$-\varpi(\bar{\gamma} - 1) + \lambda_2 \sum_{i=1}^{n} \delta_i^2 + \varepsilon\Upsilon\Upsilon^T < 0$$

which implies that the upper bound of $\mathbb{E}\{\|\tilde{z}(k)\|^2\}$ is less than ϖ. Furthermore, the decay rate of the estimation error in mean square is $\bar{\gamma}^{-1}$. Therefore, the minimization of the decay rate can be derived by maximizing $\bar{\gamma}$ which is equivalent to the condition (35). The proof is complete. ∎

Remark 5: Our main results are derived based on the LMI-based algorithm which has a polynomial time complexity. Specifically, the number $\mathcal{N}(\varepsilon)$ of flops needed to compute an ε-accurate solution is bounded by $O(\mathcal{M}\mathcal{N}^3 \log(\mathcal{V}/\varepsilon))$, where $\mathcal{M}$ is the total row size of the LMI system, $\mathcal{N}$ is the total number of scalar decision variables, $\mathcal{V}$ is a data-dependent scaling factor, and ε is relative accuracy set for algorithm. As such, the computational complexities of the established result can be represented as $O(n^7)$. Obviously, such a computational complexity depends polynomially on the variable dimensions. Nevertheless, research on LMI optimization is a very active area in the applied math, optimization and the operations research community, and substantial speed-ups can be expected in the future.

IV. AN ILLUSTRATIVE EXAMPLE

To verify the effectiveness of the proposed estimation schemes, a simulation example is conducted based on a high-speed train with 6 cars. The parameters are given in Table I, which are chosen from the experimental results of the Japanese Shinkansen high speed train [16]. The parameters of the CSMA protocol are selected to be $p = 0.5$, $\underline{N} = 1$ and $\overline{N} = 3$.

Symbol	Value	Unit
m_1, m_6	80×10^3	kg
m_2, m_3, m_4, m_5	40×10^3	kg
k	80×10^3	$\text{N} \cdot \text{m}^{-1}$
ϑ	1	m
l	20	m
T	0.1	s

TABLE II

CONTROL COMMANDS OF THE HIGH SPEED TRAIN

Commands	Samples (0.1s)	Traction force(N)
Command 1	$0 \to 3000$	$\tilde{u}_1(k) = \tilde{u}_6(k) = 2.8 \times 10^4$
		$\tilde{u}_i(k) = 1.4 \times 10^4 \ (i = 2, 3, 4, 5)$
Command 2	$3000 \to 6250$	$\tilde{u}_1(k) = \tilde{u}_6(k) = 2.48 \times 10^4$
		$\tilde{u}_2(k) = 1.24 \times 10^4 \ (i = 2, 3, 4, 5)$
Command 3	$6250 \to 9920$	$\tilde{u}_1(k) = \tilde{u}_6(k) = -0.28 \times 10^4$
		$\tilde{u}_2(k) = -0.14 \times 10^4 \ (i = 2, 3, 4, 5)$

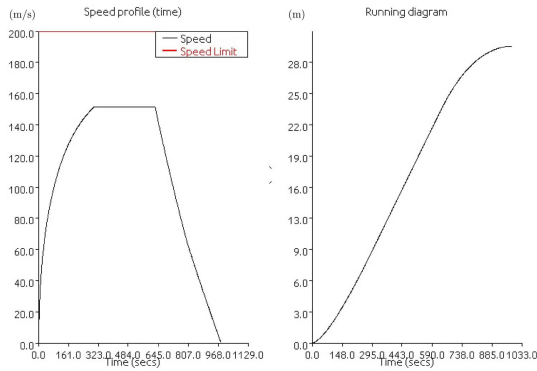
Fig. 4. The position and velocity trajectories by BRaVE simulator ($\tilde{x}_1(k)$ and $\hat{x}_1(k)$).

The matrices $\tilde{C}$ and $\tilde{M}$ are selected to be $\tilde{C} = \text{diag}\{10^{-3}I, 3.6I\}$ and $\tilde{M} = \text{diag}\{0.01I, 0.1I\}$. The covariance of the noise $\omega(k)$ is chosen as $\Omega = \text{diag}\left\{10^{-6}I, 3.6^2I\right\}$. Let the sampling period be 0.1s. The corresponding control commands are presented in Table II.

Based on the given parameters and control commands, the simulation about the position and velocity trajectories is given in Fig. 4 by using the simulator BRaVE, which is a comprehensive railway simulator developed by the Birmingham railway research and education center at the university of Birmingham in the UK.

First, let us consider Optimization Problem 1 with the given decay rate $\theta = 0.98$. By applying Corollary 1, the minimization problem (26) subject to the inequality constraints (23)-(25) can be solved and the estimator gain matrix is given in the box on the bottom of next page.

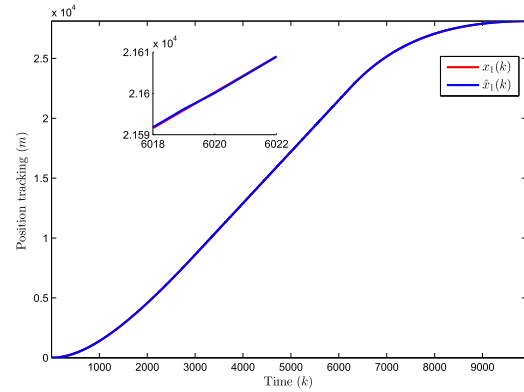Using the Matlab software, the simulation results about the estimation issue are shown in Figs. 5-8,

Fig. 5. The position tracking trajectories ($\tilde{x}_1(k)$ and $\hat{x}_1(k)$).
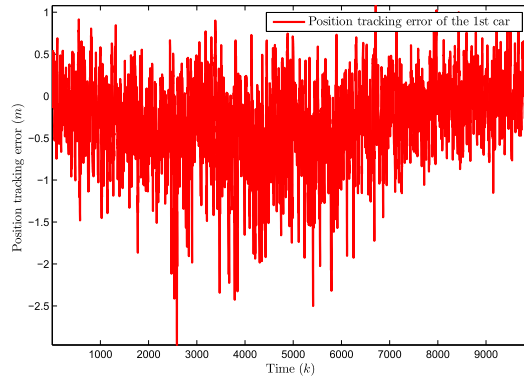
Fig. 6. The position tracking error ($e_1(k)$).
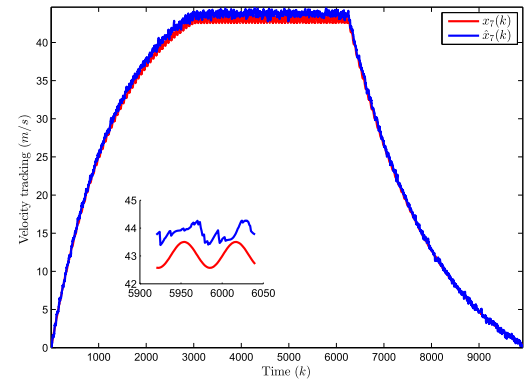
Fig. 7. The velocity tracking trajectories $\tilde{x}_7(k)$ and $\hat{x}_7(k)$.

where Fig. 5 and Fig. 7 plot the position tracking trajectories and velocity tracking trajectories, respectively. Fig. 6 and Fig. 8 show the position tracking errors and velocity tracking errors of the train, respectively. Obviously, the simulation results of the position and velocity trajectories are very close to the simulation results obtained by simulator BRaVE which implies that the train model developed in this paper indeed characterizes the dynamic behavior of the train to a satisfactory precision.

Conventionally, the information about the position and velocity is always measured by the combination of balises and speed odometers. The ZC would receive such information via

This article has been accepted for inclusion in a future issue of this journal. Content is final as presented, with the exception of pagination.

10

IEEE TRANSACTIONS ON INTELLIGENT TRANSPORTATION SYSTEMS
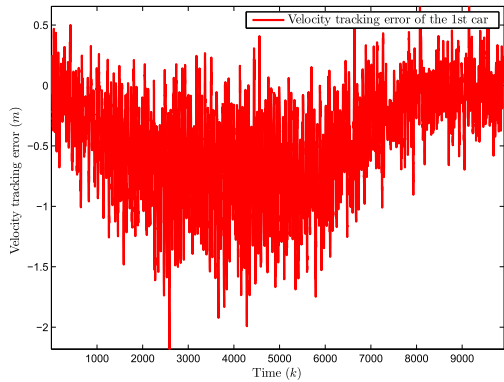
Fig. 8.　The velocity tracking error ($e_7(k)$).

TABLE III

ACCURACY COMPARISON RESULTS

	Tracking errors ($\sum_{k=0}^{9920} \|\tilde{z}(k)\|^2$)
Direct measurements	1705.6
Estimation scheme	263.1801

network-based communication. The tracking errors associated with the direct measurements and our proposed estimation scheme are shown in Table III. Obviously, the estimation scheme presented in this paper could improve the accuracy of the information about the position and velocity.

Next, let's show the improvement on the headway time. As we have discussed in Section. II-B, the headway time H_T could be calculated as follows:

$$H_T = \frac{L_{train} + L_{error} + L_{reaction} + L_{brake} + L_{safe}}{v_{\max}}.$$

The safety margin is selected from [5] as follows: $L_{safe} = 50$. The brake distance is given by $L_{brake} = \frac{v_{\max}^2}{2b}$ where b is the deceleration rate. $L_{reaction}$ is the train running distance during the reaction time of on-board system. A reasonable values of $L_{reaction}$ is given by $L_{reaction} = v_{\max}T_{reaction}$ where $T_{reaction}$ denotes the reaction time of on-board system. Assume the reaction time of on-board system is 1 second (i.e. $T_{reaction} = 1s$).

TABLE IV

HEADWAY TIME COMPARISON RESULTS

Maximum speed $v_{\max}$ (km/h)	64.857	81.071	97.285	113.499
H_T (Direct measurements)	40.309	37.004	35.003	34.124
H_T (Estimation scheme)	33.309	31.362	30.049	29.113

The headway time with the direct measurements and our proposed estimation scheme are shown in Table IV. It can be observed from Table IV that our proposed estimation scheme could significantly reduce headway time H_T.

V. CONCLUSION

This paper has addressed the state estimation problem for a train with n cars linked by couples. The dynamics of the train has been modeled by a continuous-time system and then reformulated as a discrete-time system. Considering the data transmission of the train-ground communication, the transmission behavior of the train subject to the p-persistent CSMA protocol has been described by a Bernoulli distributed sequence whose probability distribution is dependent on the number of competing nodes (trains). The corresponding state estimator has then been developed to generate the estimate of states. A sufficient condition has been derived to guarantee the ultimate boundedness of estimation error in mean square. In order to calculate the desired estimator gains under different requirements, two optimization problems have been solved to obtain the minimum of the asymptotic bound and the decay rate, respectively. A simulation example has been used to illustrate the effectiveness of the proposed design method. Further research topics include the extension of the main results to: 1) the state estimation problem for CBTC systems with time-varying parameters; 2) the fault tolerant filtering for CBTC systems subject missing measurements; and 3) the control for CBTC systems with unmodeled dynamics [17].

REFERENCES

[1] M. Basin and J. J. Maldonado, "Optimal mean-square state and parameter estimation for stochastic linear systems with Poisson noises," *Inf. Sci.*, vol. 197, pp. 177–186, Aug. 2012.

$$K = \begin{bmatrix}
185.6246 & 111.0990 & 81.3980 & 55.0893 & 51.2714 & 37.4185 & 0.0056 & 0.0015 & 0.0005 & -0.0001 & 0.0002 & 0.0007 \\
106.7411 & 157.1306 & 105.4820 & 70.3985 & 54.0893 & 31.2701 & 0.0012 & 0.0064 & 0.0005 & 0.0000 & -0.0001 & 0.0001 \\
60.6869 & 98.4843 & 159.3407 & 103.1487 & 68.2454 & 37.5287 & 0.0011 & -0.0003 & 0.0059 & -0.0003 & -0.0002 & 0.0007 \\
37.5243 & 68.2405 & 103.1544 & 159.3371 & 98.4892 & 60.6898 & 0.0007 & -0.0002 & -0.0003 & 0.0059 & -0.0003 & 0.0011 \\
31.2678 & 54.0902 & 70.4012 & 105.4870 & 157.1327 & 106.7408 & 0.0001 & -0.0001 & 0.0000 & 0.0005 & 0.0064 & 0.0012 \\
37.4227 & 51.2692 & 55.1015 & 81.3948 & 111.1046 & 185.6200 & 0.0007 & 0.0002 & -0.0001 & 0.0005 & 0.0015 & 0.0056 \\
13.1934 & 25.6005 & 20.5542 & 19.4957 & 15.5023 & 12.5453 & 0.0262 & -0.0068 & -0.0018 & -0.0003 & 0.0023 & 0.0041 \\
32.6444 & -5.0637 & 25.6867 & 15.3862 & 18.5095 & 16.0706 & -0.0099 & 0.0554 & -0.0085 & -0.0041 & -0.0019 & -0.0036 \\
25.3634 & 23.1113 & -3.5958 & 20.5772 & 21.0055 & 19.0684 & -0.0085 & -0.0073 & 0.0569 & -0.0059 & -0.0036 & -0.0065 \\
19.0572 & 21.0461 & 20.5142 & -3.5314 & 23.0700 & 25.3801 & -0.0065 & -0.0036 & -0.0059 & 0.0569 & -0.0073 & -0.0085 \\
16.0650 & 18.5500 & 15.3193 & 25.7547 & -5.1082 & 32.6582 & -0.0036 & -0.0019 & -0.0041 & -0.0085 & 0.0554 & -0.0099 \\
12.5558 & 15.4636 & 19.5560 & 20.4897 & 25.6408 & 13.1819 & 0.0041 & 0.0023 & -0.0003 & -0.0018 & -0.0068 & 0.0262
\end{bmatrix}.$$

This article has been accepted for inclusion in a future issue of this journal. Content is final as presented, with the exception of pagination.

ZOU *et al.*: STATE ESTIMATION FOR CBTC SYSTEMS WITH CSMA PROTOCOL

11

[2] B. Bu, F. R. Yu, and T. Tang, "Performance improved methods for communication-based train control systems with random packet drops," *IEEE Trans. Intell. Transp. Syst.*, vol. 15, no. 3, pp. 1179–1192, Jun. 2014.

[3] R. Caballero-Águila, A. Hermoso-Carazo, and J. Linares-Pérez, "Optimal state estimation for networked systems with random parameter matrices, correlated noises and delayed measurements," *Int. J. Gen. Syst.*, vol. 44, no. 2, pp. 142–154, 2015.

[4] H. Jiang, V. C. M. Leung, C, Gao, and T. Tang, "MIMO-assisted handoff scheme for communication-based train control systems," *IEEE Trans. Veh. Technol.*, vol. 64, no. 4, pp. 1578–1590, Apr. 2015.

[5] W. Li, T. Tang, and D. Liang, "Impact of wireless communication delay on train headway of communication based train control system," in *Proc. 19th Int. Conf. Intell. Transp. Syst.*, Rio de Janeiro, Brazil, Nov. 2016, pp. 360–365.

[6] J. Linares-Pérez, R. Caballero-Águila, and I. García-Garrido, "Optimal linear filter design for systems with correlation in the measurement matrices and noises: Recursive algorithm and applications," *Int. J. Syst. Sci.*, vol. 45, no. 7, pp. 1548–1562, Apr. 2014.

[7] R. D. Pascoe and T. N. Eichorn, "What is communication-based train control?" *IEEE Veh. Technol. Mag.*, vol. 4, no. 4, pp. 16–21, Dec. 2009.

[8] X. Qing, H. R. Karimi, Y. Niu, and X. Wang, "Decentralized unscented Kalman filter based on a consensus algorithm for multi-area dynamic state estimation in power systems," *Int. J. Electr. Power Energy Syst.*, vol. 65, pp. 26–33, Feb. 2015.

[9] M. Tabbara and D. Nešić, "Input–output stability of networked control systems with stochastic protocols and channels," *IEEE Trans. Autom. Control*, vol. 53, no. 5, pp. 1160–1175, Jun. 2008.

[10] W. Sun, F. R. Yu, T. Tang, and B. Bu, "Energy-efficient communication-based train control systems with packet delay and loss," *IEEE Trans. Intell. Transp. Syst.*, vol. 17, no. 2, pp. 452–468, Feb. 2016.

[11] H. Wang, F. R. Yu, L. Zhu, T. Tang, and B. Ning, "Finite-state Markov modeling for wireless channels in tunnel communication-based train control systems," *IEEE Trans. Intell. Transp. Syst.*, vol. 15, no. 3, pp. 1083–1090, Jun. 2014.

[12] Y. Wang, A. Ahmed, B. Krishnamachari, and K. Psounis, "IEEE 802.11p performance evaluation and protocol enhancement," in *Proc. IEEE Int. Conf. Veh. Electron. Saf. (ICVES)*, Sep. 2008, pp. 317–322.

[13] T. Wen, X. Lyu, D. Kirkwood, L. Chen, C. Constantinou, and C. Roberts, "Co-simulation testing of data communication system supporting CBTC," in *Proc. IEEE 18th Int. Conf. Intell. Transp. Syst.*, Las Palmas, Spain, Sep. 2015, pp. 2665–2670.

[14] T. Wen, C. Constantinou, L. Chen, Z. Tian, and C. Roberts, "Access point deployment optimization in CBTC data communication system," *IEEE Trans. Intell. Transp. Syst.*, vol. 19, no. 6, pp. 1985–1995, Jun. 2018, doi: 10.1109/TITS.2017.2747759.

[15] T. Wen, L. Zou, J. Liang, and C. Roberts, "Recursive filtering for communication-based train control systems with packet dropouts," *Neurocomputing*, vol. 275, pp. 948–957, Jan. 2018.

[16] C. Yang and Y. Sun, "Mixed $\mathcal{H}_2/\mathcal{H}_\infty$ cruise controller design for high speed train," *Int. J. Control*, vol. 74, no. 9, pp. 905–920, Jun. 2001.

[17] X. Zhang, X. Liu, and Y. Li, "Adaptive fuzzy tracking control for nonlinear strict-feedback systems with unmodeled dynamics via backstepping technique," *Neurocomputing*, vol. 235, pp. 182–191, Apr. 2017.

[18] L. Zhu, F. R. Yu, B. Ning, and T. Tang, "Cross-layer handoff design in MIMO-enabled WLANs for communication-based train control (CBTC) systems," *IEEE J. Sel. Areas Commun.*, vol. 30, no. 4, pp. 719–728, May 2012.

[19] L. Zhu, F. R. Yu, B. Ning, and T. Tang, "Handoff performance improvements in MIMO-enabled communication-based train control systems," *IEEE Trans. Intell. Transp. Syst.*, vol. 13, no. 2, pp. 582–593, Jun. 2012.

[20] L. Zhu, F. R. Yu, and B. Ning, "A seamless handoff scheme for train-ground communication systems in CBTC," in *Proc. IEEE VTC-Fall*, Ottawa, ON, Canada, Sep. 2010, pp. 1–5.

[21] L. Zhu, F. R. Yu, T. Tang, and B. Ning, "An integrated train–ground communication system using wireless network virtualization: Security and quality of service provisioning," *IEEE Trans. Veh. Technol.*, vol. 65, no. 12, pp. 9607–9616, Dec. 2016.

[22] L. Zhu, F. R. Yu, T. Tang, and B. Ning, "Handoff performance improvements in an integrated train-ground communication system based on wireless network virtualization," *IEEE Trans. Intell. Transp. Syst.*, vol. 18, no. 5, pp. 1165–1178, May 2017.

[23] L. Zhu, Y. He, F. R. Yu, B. Ning, T. Tang, and N. Zhao, "Communication-based train control system performance optimization using deep reinforcement learning," *IEEE Trans. Veh. Technol.*, vol. 66, no. 12, pp. 10705–10717, Dec. 2017.

[24] L. Zou, Z. Wang, H. Gao, and X. Liu, "State estimation for discrete-time dynamical networks with time-varying delays and stochastic disturbances under the Round-Robin protocol," *IEEE Trans. Neural Netw. Learn. Syst.*, vol. 28, no. 5, pp. 1139–1151, May 2017.

[25] L. Zou, Z. Wang, and H. Gao, "Set-membership filtering for time-varying systems with mixed time-delays under Round-Robin and weighted try-once-discard protocols," *Automatica*, vol. 74, pp. 341–358, Dec. 2016.

[26] L. Zou, Z. Wang, Q.-L. Han, and D. Zhou, "Ultimate boundedness control for networked systems with try-once-discard protocol and uniform quantization effects," *IEEE Trans. Autom. Control*, vol. 62, no. 12, pp. 6582–6588, Dec. 2017.

[27] L. Zou, Z. Wang, J. Hu, and H. Gao, "On $\mathcal{H}_\infty$ finite-horizon filtering under stochastic protocol: Dealing with high-rate communication networks," *IEEE Trans. Autom. Control*, vol. 62, no. 9, pp. 4884–4890, Sep. 2017.

Lei Zou received the B.Sc. degree in automation from Beijing Institute of Petrochemical Technology, Beijing, China, in 2008, the M.Sc. degree in control science and engineering from China University of Petroleum (Beijing Campus), Beijing, in 2011, and the Ph.D. degree in control science and engineering from Harbin Institute of Technology, Harbin, China, in 2016. From 2013 to 2015, he was a Visiting Ph.D. Student with the Department of Computer Science, Brunel University London, Uxbridge, U.K. He is currently a Post-Doctoral Researcher with the College of Electrical Engineering and Automation, Shandong University of Science and Technology, Qingdao, China. His research interests include nonlinear stochastic control and filtering, and networked control under various communication protocols. He is a very active reviewer for many international journals.

Tao Wen was born in Kaifeng, Henan, China, in 1988. He received the B.S. degree from Hangzhou Dianzi University, Hangzhou, China, in 2011, and the M.Sc. degree from University of Bristol, Bristol, U.K., in 2013.

He is currently pursuing the Ph.D. degree with the Birmingham Centre for Railway Research and Education, University of Birmingham, Birmingham, U.K. His research interests include CBTC system optimization, railway simulator development, railway dependability improvement, and signal processing.
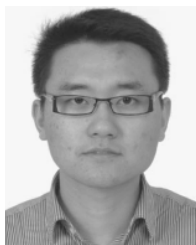
Zidong Wang (SM'03–F'14) was born in Yangzhou, Jiangsu, China, in 1966. He received the B.Sc. degree in mathematics from Suzhou University, Suzhou, China, in 1986, and the M.Sc. degree in applied mathematics and the Ph.D. degree in electrical engineering from Nanjing University of Science and Technology, Nanjing, China, in 1990 and 1994, respectively.

From 1990 to 2002, he held the teaching and research appointments at universities in China, Germany, and U.K. He is currently a Professor of dynamical systems and computing with the Department of Information Systems and Computing, Brunel University, U.K. He has published over 300 papers in refereed international journals. His research interests include dynamical systems, signal processing, bioinformatics, and control theory and applications. He received the Alexander von Humboldt Research Fellowship of Germany, the JSPS Research Fellowship of Japan, and the William Mong Visiting Research Fellowship of Hong Kong.

Dr. Wang is a fellow of the Royal Statistical Society and a member of the Program Committee for many international conferences. He serves as an Associate Editor for 12 international journals, including IEEE TRANSACTIONS ON AUTOMATIC CONTROL, IEEE TRANSACTIONS ON CONTROL SYSTEMS TECHNOLOGY, IEEE TRANSACTIONS ON NEURAL NETWORKS, IEEE TRANSACTIONS ON SIGNAL PROCESSING, and IEEE TRANSACTIONS ON SYSTEMS, MAN, AND CYBERNETICS.

This article has been accepted for inclusion in a future issue of this journal. Content is final as presented, with the exception of pagination.

12   IEEE TRANSACTIONS ON INTELLIGENT TRANSPORTATION SYSTEMS

Lei Chen received the B.Eng. degree in automation engineering from Beijing Jiaotong University, Beijing, China, in 2005, and the Ph.D. degree in railway traffic management from University of Birmingham, Birmingham, U.K., in 2012. His research interests include railway traffic management and control, railway safety critical system design, and railway simulation. He is currently a Birmingham Fellow for railway traffic management with the Birmingham Centre for Railway Research and Education, University of Birmingham.

Clive Roberts is the Director of the Birmingham Centre for Railway Research and Education, which is the largest railway research group in Europe with just over 100 researchers. He is currently a Professor of railway systems with University of Birmingham. He works extensively with the railway industry and academia in Britain and overseas. He leads a broad portfolio of research aimed at improving the performance of railway systems, including a leading strategic partnership in the area of data integration with Network Rail. His main research interests lie in the areas of railway traffic management, condition monitoring, energy simulation, and system integration.